Literature Review

Chapter 2

2. Literature Review

2.1. Current therapies for AD

The currently available pharmacotherapies of AD include AChE and NMDA receptor antagonists. At present, there is no cure for AD, and FDA-approved drugs for AD management are also sufferings from severe side effects. Acetylcholinesterase (AChE) has emerged as a promising drug target for the treatment of AD. Butyrylcholinesterase (BChE), a closely related enzyme to AChE, is also responsible for the regulation of cholinergic neurotransmission by hydrolyzing ACh [76]. Recent studies suggest that brain-targeted BChE not only lowers Aβ levels in transgenic mice but also improves cognitive performance in animals [77]. The level of both AChE and BChE changes dramatically as the disease progresses. Therefore, both enzymes have been explored for neuroprotective and disease-modifying therapy for AD.

2.1.1. Cholinesterase inhibitors (ChEIs)

The currently available treatments in the market for AD can be classified into two classes, namely AChE inhibitors and NMDA receptor (N-methyl-D-aspartate) antagonists [78]. Apart from the reversible and selective AChE inhibitors donepezil (DPZ) (**1**) and galantamine (**2**), the pseudo-irreversible AChE and BChE inhibitor rivastigmine (**3**), a carbamate derivative, with slight selectivity towards BChE, is also available for AD (Figure 2.1). Donepezil (Aricept) a FDA-approved drug for the treatment of AD, which came into the market in 1996 [79]. DPZ has been considered a safe and well-tolerated drug. It interacts with the active site as well as PAS of the AChE through aromatic interactions. The *N*-benzyl piperidine and indanone groups of DPZ interact with Trp84 of the anionic subsite and indole ring of Trp279 at the peripheral site of the enzyme, respectively. The pharmacological profile of DPZ develops the interest for the generation

of other *N*-benzylpiperidine derivatives as potential anti-AD agents. DPZ appears to be a safe druggable profile probably due to its novel *N*-benzylpiperidine structure. Galanthamine is an alkaloid isolated from the family *Amaryllidaceae*. Galanthamine acts as a competitive and reversible inhibitor of AChE. It also allosterically interacts with nicotinic acetylcholine receptors (nAChR) and increases the release of ACh. Galanthamine (**2**) is less potent (IC_{50} = 800 nM); however, its unique dual interaction and less toxic effects lead to the development of novel potent analogs. Rivastigmine (**3**) is a new generation carbamate derivative and covalent inhibitor of AChE. It is a pseudo irreversible inhibitor of ChEs. It exhibits a ten-fold greater affinity for brain AChE than for the peripheral one, although it is a weak inhibitor of AChE. Apart from this, tacrine (**5**) was the first licensed cholinesterase inhibitor to be approved for AD care in 1993, but it was withdrawn from the market due to its poor efficiency in modifying/reversing pathological disruption, disease progression, and associated adverse effects such as hepatotoxicity [80]. These drugs provide only symptomatic treatment for the initial 1-2 years of onset of the symptoms without addressing the underlying pathophysiological factors responsible for the neurodegeneration. These approved drugs are unable to compensate for the neuronal loss in the later stages of the disease; therefore, the pharmacological action and efficacy are limited to the early stages of AD.

2.1.2. Noncompetitive N-methyl-D-aspartate (NMDA) antagonists

Memantine (1-amino-3,5-dimethyladamantane), an amino-alkyl cyclohexane derivative, was first synthesized by Eli Lilly and Company (Indianapolis, IN) and patented in 1968. Memantine, an ionotropic non-competitive NMDA receptor antagonist, is approved for use in moderate to severe AD [81]. It is the only NMDA antagonist that is clinically prescribed to provide symptomatic relief and enhance the life quality of AD patients. However, memantine possesses limited clinical

efficacy with side effects such as dizziness, occasional restlessness/agitation, constipation, ocular effects, confusion, rash, and urinary incontinence [82]. At present, a 2nd generation memantine derivatives are currently in development and have better neuroprotective properties than memantine [83].

Aducanumab (Aduhelm) is a amyloid beta (Aβ) directed monoclonal antibody used to treat AD. It directly target aggregated Aβ fibrils and disintegrate them to smaller non toxic filaments. It was approved in June 2021 by US-FDA, and is used to treat mid cognitive imapiremnt or mild dementia stage of AD. Suvorexant (Belsomra) is a orexin receptor antagonist used for the treatment of insomnia. It was approved for sale by US-FDA in august 2014. It is not recommended in people diagnosed with narcolepsy, liver imparement and pregnancy.

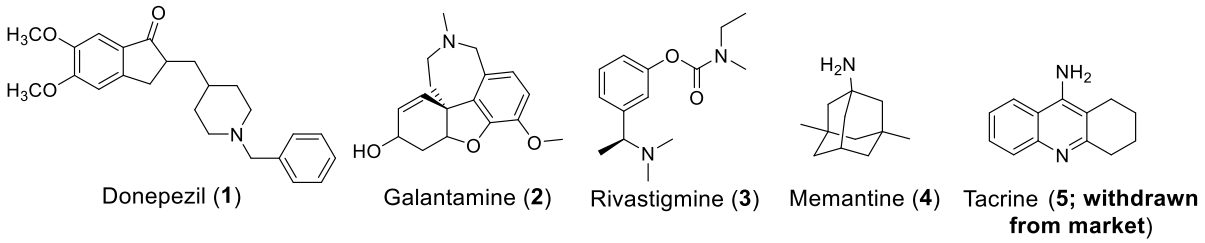

Figure 2.1. Chemical structures of the drugs for the treatment of AD.

2.2. Antioxidant therapy for AD

Oxidative stress (OS) has been strongly implicated as a significant contributing factor responsible for neurodegeneration in AD. One of the early events in the neurodegeneration pathway related to AD is increased oxidative stress [84, 85]. The key role played by OS in AD pathogenesis is well established in the literature [86]. Oxidative stress is defined as dyshomeostasis between ROS/RNS and the cells' antioxidant ability to neutralize them. It is caused either by producing reactive oxygen species (ROS) or due to failure in the elimination of ROS [87]. OS arises due to an imbalance that occurs at a molecular/cellular level when free radical production exceeds antioxidant scavenging capacity [85, 88]. The electrons leaked from the mitochondrial membrane react with oxygen to

form superoxide anions ($O_2^{\cdot-}$). These superoxide radicals further react and generate other ROS forms like hydrogen peroxide (H_2O_2) and hydroxyl ion (OH^-). Whereas ROS like superoxide ($O_2^{\cdot-}$) and H_2O_2 interacts with nitric oxide (NO) to generate peroxynitrite anion (RNS). Overproduction of reactive species (ROS/RNS) leads to compromised antioxidant function and induces toxicity *via* lipid peroxidation, oxidation of proteins, DNA, and RNA damage [89]. Overproduction of ROS/RNS is highly reactive towards nucleic acid, proteins, lipid, and other molecules in the brain, which governs the principle factors in the progressive neuronal damage in AD's pathophysiology [90]. In AD, overproduction of ROS in neurons is likely to be associated with significantly increased oxidative damage and mitochondrial dysfunction [91, 92].

Natural products are the major sources of therapeutic agents for diseases, including neurodegenerative disorders [93]. There are a variety of natural constituents, including caffeic acid (CAA; **7**), curcumin (**8**), cinnamic acid (CIA; **9**), kaempferol (**10**), butein (**11**) sharing the ferulic acid (**FA, 6**) structural motif that can provide neuroprotection under neurodegenerative conditions as shown in figure 2.2. Polyphenols constitute one of the most important groups of natural metabolites of plants. In their structural architecture, these natural moieties harbor a common fragment present in **FA**, *i.e.* trans-alkene attached to a phenyl ring bearing a hydroxyl group, as the key structural feature that decodes the potential of **FA** scaffold in ameliorating Aβ neurotoxicity through a variety of mechanisms. CAA's preclinical pharmacological studies revealed a protective effect in hyperinsulinemia rats against AD pathogenesis via modulating cerebral insulin signaling, Aβ accumulation, and synaptic plasticity [94]. Numerous review articles and research work have been published that corroborated the potential of curcumin [95-98], CIA [99, 100], kaempferol [101-103], and butein [104, 105] based derivatives in diagnosis, prevention, and treatment of AD in *in-vitro* and *in-vivo* biological investigation [106].

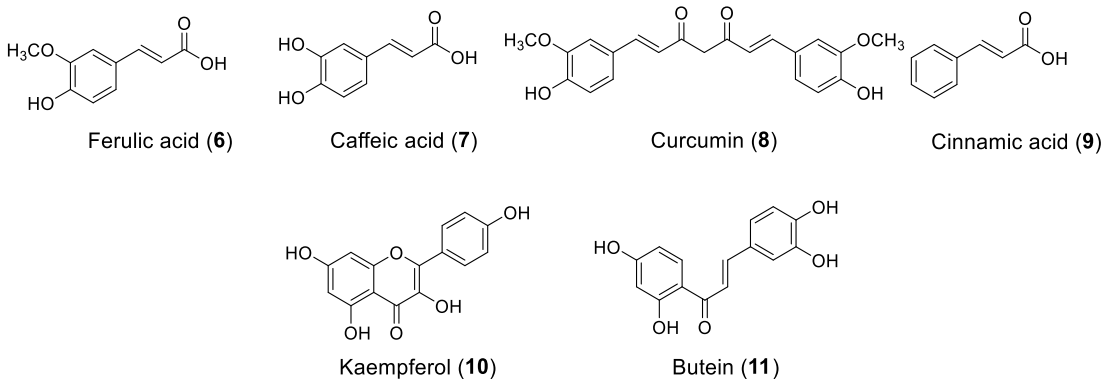

Figure 2.2. Chemical structures of the natural products are known for the anti-AD effect.

2.3. Ferulic acid (FA) and AD

Ferulic acid (4-hydroxy-3-methoxy cinnamic acid) is a naturally occurring aromatic α-β unsaturated compound, first isolated from *Ferula foetida* (Figure 2.2) abundantly present in agriculture waste. **FA** is produced during the biosynthesis of lignin from tyrosine or phenylalanine [107]. **FA** has been widely used as an antioxidant for fats in food industries. It is the most common active component of traditional Indian medicine reported for anti-inflammatory, antioxidant [108], inhibition of Aβ aggregation, and protects the neuronal cells from oxidative damage [109]. Furthermore, **FA** inhibits various cytotoxic enzymes' upregulation, including cyclooxygenase (COX), caspases, and nitric oxide synthase. It also upregulates different cytoprotective enzymes such as threonine kinase and heme oxygenase-1 [110].

FA possesses structural motifs that contribute to the free radical scavenging capability of this compound. Electron-donating groups such as 3-methoxy and the 4-hydroxyl group on the benzene ring of **FA** are hypothesized to produce an antioxidant effect. Whereas other functional groups like the terminal –COOH group adjacent to unsaturated C-C double bond act as an anchor in the binding of **FA** to the lipid bilayer, thereby protecting against lipid peroxidation [111]. **FA** has shown promising neuroprotection in *in-vitro* studies. However, the literature reports and recent

research work from our laboratory have strongly implicated that **FA** does not effectively interact with AChE and BChE (<20% inhibition of AChE and BChE at 20 mM) [112]. Furthermore, relatively low lipophilicity (cLog P ~1.5), poor blood-brain barrier (BBB) permeability and poor aqueous solubility are thought to be major limitations associated with **FA** a druggable agent for AD [112-114].

It is a well-established fact in the literature that Aβ plaque deposition contributes to AD neuropathology [115]. These plaques formation in the brain induces neuro-inflammation and radical generation, which ultimately leads to neurodegeneration in brain regions such as the hippocampus and cortex [116]. In *in-vitro* Aβ aggregation studies, it has been shown that **FA** not only destabilizes the aggregated Aβ fibrils but also inhibits the formation of Aβ aggregates [117]. Furthermore, **FA** protects the brain from Aβ toxicity and decreases Aβ deposition in the AD mice model [118]. Chronic administration of **FA** to the transgenic mouse model of AD could enhance learning and memory and reduce the toxic Aβ fibrils level [119]. **FA** also inhibits the activation of astrocytes and microglia induced by Aβ aggregates [120]. Further, it protects the neuronal cells against Aβ mediated oxidative stress. Intriguingly, the oral administration of **FA** did not significantly affect *in-vivo* Aβ modulation [121, 122].

Given the significant role of **FA** *via* regulating oxidative stress and capable of reducing aggregated Aβ species load in AD pathogenesis, **FA** is still not druggable and suffers from several shortcomings that limit its application as an anti-AD agent [123]. To overcome these limitations, various research groups developed novel molecules encompassing **FA** as a template and carried out the appropriate structural modifications to improve its drug properties [124]. Interestingly, **FA**'s structure provides significant structural transformation space to improve upon the drawbacks associated with this. **FA** can be used as a template, which is structurally similar to aforesaid several

naturally containing trans-alkenes attached to the phenyl ring for further investigation against AD. The presence of acid and phenolic functional groups in **FA** provides the chemical space for multiple structural modifications to introduce the appropriate chemical appendage to convert it into a druggable molecule. It is worth mentioning that majority of the structural modification reported on **FA** template in the literature for the management of AD are focused around these functional (phenolic and acid) groups to bring a balance of hydrophilicity/lipophilicity, improvement in cholinergic inhibition, and lipid solubility while retaining its inherent properties [125, 126].

2.4. FA as a potential therapeutic agent for AD

2.4.1. Water-soluble ferulic acid (FA) derivatives

FA is well known in the literature for therapeutic properties such as potent antioxidant, anti-inflammatory, anticancer, modulator of Aβ-induced neurotoxicity, and enhanced learning/memory deficit in animal models [118, 127, 128]. Given the vast therapeutic potential, **FA** gains its widespread use in the cosmetics, and pharmaceutical industries, however, its applicability as a drug is constrained due to its low water solubility and sluggish entry into the brain. To improve the water solubility of **FA**, Kikugawa *et al.* [113, 129] designed and synthesized water-miscible **FA** glycerol and diglycerol derivatives *i.e.,* **12** and **13** (Figure 2.3**)** using **FA** esterase from *Aspergillus niger*. Interestingly, **12** was found to be five folds higher water-miscible than parent compound **FA** whereas **13** turnouts to be higher water solubility than glycerol derivative **12**. Further, these derivatives were evaluated for neuroprotection property towards Aβ-induced neurotoxicity on the cortical neurons. Despite these structural modifications, both derivatives impeded the aggregation of the Aβ species and destabilized preformed Aβ fibrils aggregates, which was further confirmed in $A\beta_{25–35}$ induced neurotoxicity studies in the neuronal cells. The

equipotent antioxidant property of **12** and **13,** compared to **FA,** revealed the contribution of antioxidant activity to the neuroprotective effect. The water-soluble **FA** derivatives, **12** and **13,** resisted the development of Aβ aggregates. They destabilized the aggregation of Aβ fibrils in *in-vitro,* which suggests the therapeutic potential of **12** and **13** to halt AD development by directly inhibiting aggregation of Aβ species in the brain, rather than scavenging the ROS. Interestingly, **12** and **13** were orally administered to mice with food and water, followed by monitoring the hippocampus neuronal cell death. The result of this study demonstrated that **12** and **13** could improve Aβ induced dysmnesia (an impaired memory characterized by the inability to learn simple new skills) in parallel with exerting neuroprotective effects in the hippocampal region. Similarly, **12** and **13** were also shown to enter the hippocampus and protect the neuronal cell against Aβ-induced cytotoxicity. The water-soluble **FA** derivatives displayed no cytotoxicity up to 2 mM.

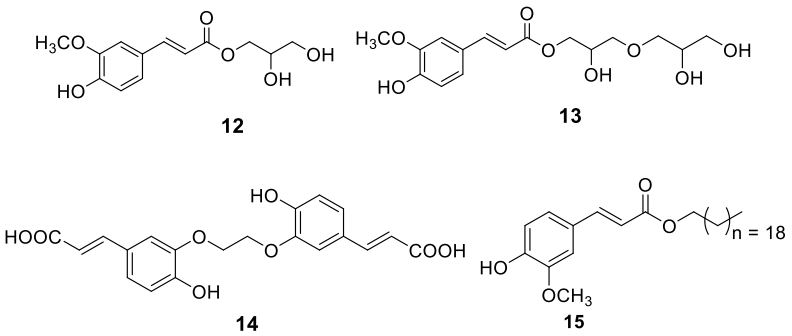

Figure 2.3. Structures of novel ferulate ester derivatives with improved water solubility and potency in AD model.

2.4.2. Dimeric derivative of FA

In 2016, Jung *et al.,* [130] designed and synthesized a novel **FA** dimeric derivative, **14** (Figure 2.3) based on the premise that dimerization of **FA** could raise the pharmacological efficiency *via* divalent and multivalent binding interactions within the active sites located on pathogenic Aβ oligomer. The protective effect of **14** was evaluated in two murine models of AD *i.e.* a mouse

model of an intra-cerebroventricular (ICV) injection of $A\beta_{1-42}$ and a transgenic (Tg) APP/PSI mouse model. In the former model, the mice were pretreated with **14** (30 mg/kg/day; intra-gastric) for five days; after that, the passive avoidance performance and Y maze test were carried out. It is noteworthy that **14** could efficiently reverse the $A\beta_{1-42}$ induced memory impairment in both the AD models. Whereas a lower dose of **14** (10 mg/kg) for 5-day did not produce a statistically significant efficacy. In APP/PSI AD model, **14** (3 and 30 mg/kg/day) was administered to the mice *via* drinking water for three months. After 1.5 and 3 months, the novel object recognition test was carried out, and results revealed that treatment with **14** significantly improved novel object recognition memories at both time phases *i.e.,* 1.5 and 3 months. Furthermore, the quantitative estimation of $A\beta_{1-42}$, $A\beta_{1-40}$ and IL1-β in the frontal cortex of these mice demonstrated the ability of **14** to reduce the cortical levels of $A\beta_{1-40}$ and $A\beta_{1-42}$ in the cortex. Intrudingly, treatment with **14** did not change the cortical IL-1β levels, indicating its distinct mode of action. The treatment group (30 mg/kg) that survived for three months indicated the developed novel molecules' safety. The novel object recognition memory enhancement and decreased level of Aβ species suggested **14** could be safe and useful against AD.

2.4.3. Development of ferulic acid ester as a memory enhancer

Many studies reported that *Rhodiola Rosea* extract could act as a memory enhancer in rats by counteracting pharmacologically induced deflects in pre-pulse inhibition in rats and milder symptoms of depression in humans [131-133]. In 2018, Michels and colleagues reported their work to leverage the ability of the plant *Rhodiola Rosea*. They identified ferulic acid eicosyl ester, **15**, (Figure 2.3) as a key constituent responsible for memory enhancement property [134]. To investigate the memory enhancement effect of *R. Rosea* root and its extract, three insect models involving larval, adult *Drosophila melanogaster,* and honeybee *apis mellifera* were utilized. It was

observed that larval *Drosophila* exhibited improved odor-taste reward associative memory ratings in a dose-dependent manner when fed over dried root content from *R. Rosea* and prevented the age-related loss of this hunger memory in adult flies. While commercially available *R. Rosea* containing the SHR-extract (a tablet preparation was containing "arctic root" tablets, Swedish Herbal Institute) did not improve memory scores in larval Drosophila. The odor-sugar associative learning paradigm study indicated that *R. Rosea* only improved memory scores in aged *Drosophila* but not in young *Drosohilia*, suggesting that the *R. Rosea* only compensated for age-related memory decline in adult *Drosophila*. The experiments were conducted on harnessed bees suggested the feeding on *Rhodiola*^{4E} (stock solution prepared from dried *Rhodiola root*) could improve memory acquisition and memory consolidation, prior and after the training, respectively, without any effects on memory retrieval in the honey bee. The compounds found in *R. Rosea* extract, such as b-sitosterol-b-D-glucoside (BSSG) and **15** (Figure 2.3), were synthesized to identify their role in memory enhancement. In *Drosophila larvae*, **15** enhanced memory scores in a dose-dependent manner with memory scores doubled at a concentration of 0.71 μM, whereas 10-times higher or 10-times lower concentrations had no statistically significant effect in the similar experiments. Similar dose-dependency behavior was observed using *Rhodiola* extract (crude). The compound **15** enhanced CA1 neuronal excitability, responsible for learning and memory enhancement in rodents and humans, and improved contextual fear memory. The increase in the parent molecule **FA**'s lipophilicity *via* ester formation was hypothesized to make **15** accessible to cross the BBB efficiently. In conclusion, the study on *R. Rosea* plant's supplementary (extract or dried root part) diet and synthesized derivatives corroborated **15** as a memory enhancer and has the potential for clinical application in memory-associated disorders like AD.

2.5. FA hybrid molecules for AD

2.5.1. FA-Donepezil based hybrid molecules for AD

2.5.1.1. FA-alkylamine-benzylpiperidine hybrids (FAHs)

In 2016, Wei Xu and his co-workers [119] designed and generated another series of novel DPZ-**FA** hybrids with the applied MTDLs approach to manage mild to severe AD states. The developed compounds were evaluated for inhibitory potency towards ChE, antioxidant property, BBB permeability, metal chelation, and neuroprotection properties. The *in-vitro* SAR studies revealed that the compound bearing N-benzylpiperidine (NBP) coupled with **FA** at the terminal ends of the long alkyl chain spacer exhibited better ChEs inhibition activities. The compounds bearing both the OH and OCH_3 groups *i.e.* **16** and **18** (Figure 2.4) possess moderate enzyme inhibition property compared to their counter analogs with only methoxy (OCH_3) or hydroxyl (OH) group. The OH or OCH_3 group's position also influences the inhibition of AChE (**16**; IC_{50} = 0.65 ± 0.036 μM vs. **17**: IC_{50} = 1.06 ± 0.05 μM). The data showed that compound **18** exhibited moderate inhibition against ChEs (IC_{50} values of 0.39 ± 0.028 for AChE and 0.97 ± 0.10 μM for BChE) compared to control drug DPZ (IC_{50} = 0.035 ± 0.002 μM for AChE). The antioxidant activity of the developed compounds was evaluated by using ABTS (2,2′-azino-bis-3-ethylbenzothiazoline-6-sulfonic acid) radical scavenging assay using Trolox as a reference compound. The compounds **16** and **18** were found to be potent ABTS radical scavengers with 1.39 and 1.78 Trolox equivalents, respectively. The compounds having phenolic groups such as **16** and **18** could moderately scavenge free radicals suggesting the OH group of **FA** played a crucial role in exhibiting anti-oxidant activity. Based on the promising antioxidant property and potential enzymatic inhibitory activity, **18** was chosen for further therapeutic assessment. The *in-silico* studies exposed the concurrent interaction of **18** with the PAS and CAS of AChE. The di-

methoxy and OH group on the phenylpropanoid and core amide moieties were attributed to the potential metal chelating ability of **18**. It was confirmed from the BBB-parallel artificial membrane permeability assay (PAMPA) that **18** could enter the brain.

2.5.1.2. *N*-benzylpiperidine (NBP)-FA hybrid derivatives

Dias, K.S.T., *et al.*, in 2017 [135] designed, synthesized, and evaluated a series of novel feruloyl-donepezil ester derivatives by fusing the NBP, a fragment from donepezil pharmacophore accountable for AChE recognition moiety, with feruloyl subunit of **FA** and evaluated for multi-target activities for the management of AD. The studies such as *in-vitro* quantitative estimation of antioxidant activity along with metal chelation, anti-inflammatory, protective effect against ROS in the neuronal cells and protection against Aβ induced toxicity, enzyme kinetics, molecular docking, and cholinesterases inhibition activities were carried out. The *in-vitro* inhibition assay towards *electrophorus electricus* AChE (*ee*AChE) revealed **19** and **20** (Figure 2.4) as lead compounds exhibiting the highest *ee*AChE inhibitory activity with an IC_{50} value of 0.46 μM and 16.74 μM, respectively. Surprisingly, the aforesaid structural modifications were turned out to be deleterious, and the tested compounds were found to be weak ChEs inhibitors compared to DPZ (IC_{50} = 0.026 μM). The findings from *in-vitro* and *in-vivo* experiments showed that **19** has the most potent antioxidant activity *via* activating the Keap1/Nrf2/ARE in neuronal SH-SY5Y cells line. In the *in-vitro* antioxidant activity, **19** and **20** showed a steady decrease in ROS formation concentration in a concentration-dependent manner, suggesting the contribution of **19** and **20** towards ROS inhibition activity of SH-SY5Y cells. Compound **19** could effectively and selectively chelate cupric and ferrous ions over ferric and zinc cations. Compound **19** also displayed neuroprotective effects in $A\beta_{1-42}$ oligomers induced neuronal cell death and significantly reduced inflammation in formalin-induced antinociceptive and peritonitis induced by lipopolysaccharide.

2.5.1.3. FA-O-alkylamine derivatives

A series of novel **FA**-O-alkylamine derivatives was developed by Sang *et al.*, [136] as a multifunctional anti-AD agent. The structural analogs consist of the fused 4-benzylpiperidine fragment from donepezil moiety with **FA** carboxyl group *via* amidic linkage and secondary amines fragment having methylene spacer of variable lengths to the phenolic group of **FA**. Among all the compounds, **21** and **22** (Figure 2.4) demonstrated potent *ee*AChE inhibition activity with IC_{50} = 2.21 ± 0.01 μM and 2.13 ± 0.01 μM, respectively. The *in-vitro* inhibition assay supported the high selectivity of the developed compounds for *eq*BChE over *ee*AChE. Interestingly, **22** displayed potent inhibition potency towards *eq*BChE with an IC_{50} value of 0.021 ± 0.0001 μM, selectivity index (SI) value of 101, and significant anti-ROS activity with ORAC-FL value of 0.55 ± 0.01 Trolox eq. Compound **21** also displayed potent inhibition activity towards *eq*BChE with IC_{50} = 0.12 ± 0.01 μM. The inhibition potency of **22** towards *h*AChE and *h*BChE followed the same trend having more potent activity towards BChE (IC_{50} = 0.07 ± 0.01 μM and IC_{50} = 3.82 ± 0.05 μM for *h*AChE). Compound **22** in a dose-dependent manner inhibited self-induced $A\beta_{1-42}$ aggregation with maximum inhibition (68.7 ± 0.76%) at 50 μM. Surprisingly, a vast majority of the developed molecules were devoid of potent antioxidant properties in ORAC assay. Among the developed molecules, **22** was found capable of rescuing PC12 cells from oxidative stress damage caused by H_2O_2 and devoid of acute toxicity in mice up to 1000 mg/kg. The substantial reverse in scopolamine-induced memory deficit was observed in step-down passive avoidance test in mice treated with **22**.

2.5.1.4. FA-N-alkyl benzyl piperidinediamide derivative

In 2015, Benchekroun *et al.* [137] designed and developed multifunctional DPZ-**FA** hybrid derivatives that exhibited cholinesterase inhibition and antioxidants properties. These molecules

consisted of N-benzylpiperidine of DPZ and were conjugated with **FA** to produce potential inhibitors with concomitant cholinesterase inhibition with potent antioxidant property. Among these compounds, 2-chloro-6-methyl aniline fragment containing derivative **23** (Figure 2.4) exhibited the most potent *ee*AChE inhibitory activity (24.8 ± 4.1 % inhibition at 1 μM). The methoxy alkyl indole derivative **24** (Figure 2.4) with ethylene linker was turnout to be ~198 fold higher selective towards *eq*BChE with an IC_{50} value of 10.39 ± 0.48 nM compared to DPZ (IC_{50} value of 2057 ± 290 nM). Furthermore, **24** was found to be a potent antioxidant agent with ORAC value of 8.71 ± 0.20, measured using Trolox as the reference standard and fluorescein (fluorescent probe). Based on preliminary ChEs inhibitory activity and antioxidant property, **24** exhibited the most potent and selective *eq*BChE inhibitory activity along with potent antioxidant property in this series, compared to parent molecule **FA** and melatonin, showing ORAC value of 3.74 ± 0.22 and 2.45 ± 0.09 Trolox eq., respectively (Table 2.1).

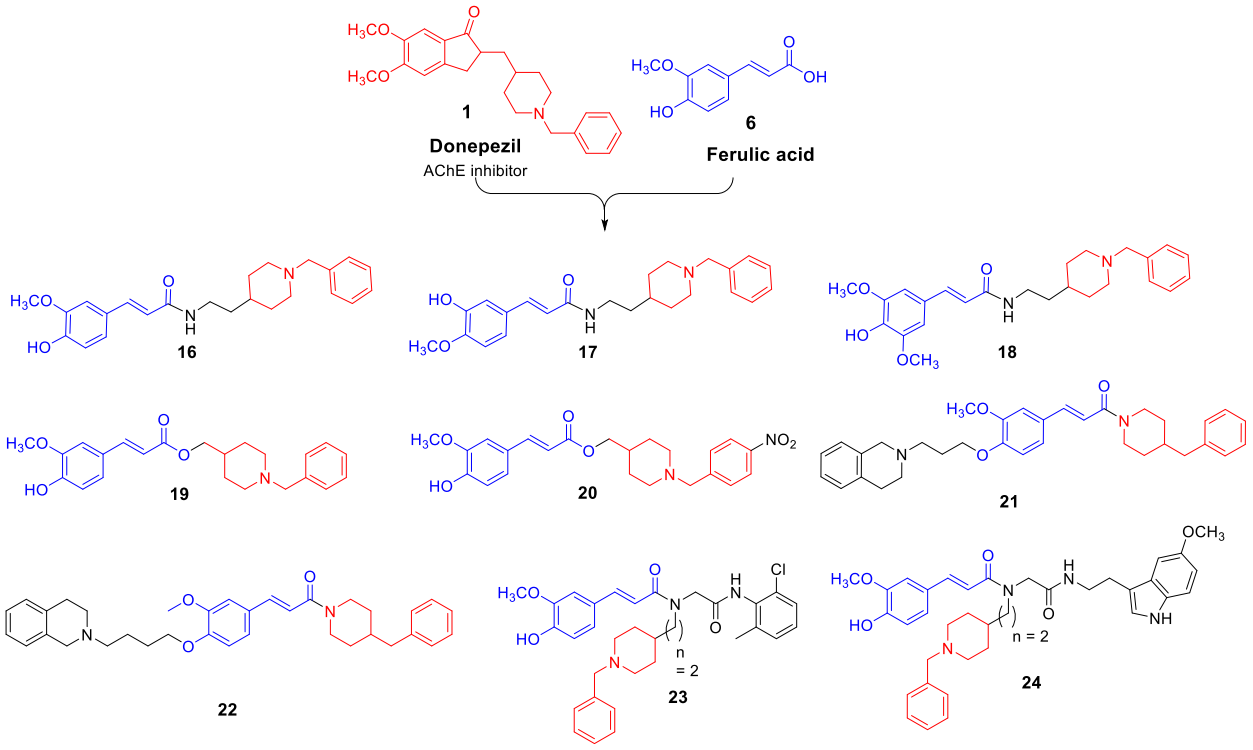

Figure 2.4. Chemical structures of ferulic acid (FA)-donepezil (DPZ) based hybrid molecules.

Table 2.1. *In-vitro* biological data for evaluating the therapeutic potential of hybrid analogs based on novel ferulic acid (**FA**)-donepezil and their mode of action in the experimental AD model.

Sr. No.	Code	**Pharmacological assessment of efficacy and safety**				**Mode of action**	**Ref.**
		Cholinesterase inhibition (IC_{50}) ± SD		**Neuroprotective activity**	**Antioxidant assay**		
		eeAChE	**eqBChE**				
1	**16-18**	0.65 ± 0.036 μM (16), 1.06 ± 0.05 μM (17), 0.39 ± 0.028 μM (18)	1.22 ± 0.15 μM (16), 2.47 ± 0.22 μM (17), 0.97 ± 0.10 μM (18)	*nd.*	DPPH Assay**= 34.1 ± 1.8** μM for 16, 764 ± 18** μM for 17 and 24.9 ± 1.4** μM for 18	ChEI activity, ABTS radical scavengers, DPPH (2,2-diphenyl-1-picrylhydrazyl) radical scavenging capacity	[119]
2	**19, 20**	0.46 μM (19), 16.74 μM (20)	24.97 μM (19)	*nd.*	DPPH Assay**= 49.41 μM for 19 and 46.66 μM for 20	ChEI activity, metal chelation, neuroprotective, antioxidant activity *via* activating the Keap1/Nrf2/ARE in neuronal SH-SY5Y cells line.	[135]
3	**21, 22**	2.21 ± 0.01 (21) 2.13 ± 0.01 (22)	0.12 ± 0.01 μM (21) 0.021 ± 0.001 μM (22)	Aβ anti-aggregation activity : 55.6% ± 2.0 for 21 at 25 μM and 31.2% ± 0.05 for 22 at 12.5 μM	ORAC value = 0.51 ± 0.01 TE for 21 and 0.55 ± 0.01 TE for 22.	ChEI activity, antioxidant, inhibition of self-induced amyloid $A\beta_{1-42}$ aggregation, protect PC12 cells from H_2O_2-induced oxidative cell injury, Substantial reverse in scopolamine-induced memory deficit.	[123]
4	**23, 24**	24.8% ± 4.1 (23)	57.3% ± 5.8 (23), 10.39 ± 0.48 nM (24)	*nd.*	ORAC value = 6.90 ± 0.39 TE for 23 and 8.71 ± 0.20 TE for 24.	ChEI activity, antioxidant property.	[137]

IC_{50}: 50% inhibitory concentration (means ± SD of three experiments), *nd.* = not determined, ee = electric eel, eq = equine, h = human and ** Data are expressed as trolox equ. (TE) compound ± SD (n = 3).

2.5.2. FA-tacrine based hybrid molecules for AD

2.5.2.1. FA-tacrine alkylenediamine hybrid molecules (TFAHs)

Fang L. *et al.*, in 2008 [138], designed and synthesized tacrine–**FA** hybrids to generate compounds with better ChE inhibitory activity compared to parent drug tacrine. Among the developed molecules, **25** exhibited the highest inhibitory activities towards AChE and BChE. The ChE inhibitory assay revealed the promising inhibitory activity towards *ee*AChE of **25** and **26** (Figure 2.5) with IC_{50} values 4.4 ± 1.7 and 9.6 ± 2.1 nM, respectively, to be higher than the parent drug tacrine (IC_{50} value 45.1 ± 6.9 nM). In case of *eq*BChE inhibition, **25** and **26** showed lower inhibition value (IC_{50} = 6.7 ± 1.6 nM and 12.7 ± 2.6 nM, respectively) compared to tacrine (IC_{50} = 5.1 ± 1.0 nM). The ORAC-fluorescein assay was used to screen all the target compounds for their protective effect against oxidative stress, and most of the molecules showed potent anti-oxidant properties compared to Trolox.

2.5.2.2. FA-tacrine-diamide side-chain derivatives

A series of **FA**-tacrine hybrid based on the multicomponent reaction was reported by M. Benchekroun and colleagues for the discovery of new MTDLs with improved efficacy and decreased side effects associated with tacrine. In 2015, this group developed novel tacrine–**FA** hybrids and evaluated their theoretical aspects (*in-silico*) and biological potency in terms of ChE inhibitory activity, hepatotoxicity profile, antioxidant profile, and ADMET profile [139]. All the synthesized 14 compounds were found to be less toxic than tacrine (cell viability 93.4 ± 4.7% in 1 μM and 34.4 ± 2.7% at 1000 μM) in the HepG2 cell hepatotoxicity assay. The lead **27** (Figure 2.5) 9-amino-7-methoxy-1, 2, 3, 4-tetrahydroacridine derivative, expectedly had a cell viability of 98.8 ± 2.4% at 1 μM and 59.4 ± 4.7% at 1000 μM. In terms of neuroprotection property with SH-SY5Y cell, **27** was devoid of toxicity up to 10 μM with cell viability 95.1 ± 1.4. Compound **27** exhibited

inhibitory property with IC_{50} value 22.2 ± 1.6 nM, and 68.2 ± 3.9 nM towards *h*AChE and, *h*BChE, respectively. The antioxidant potential through ORAC-FL assay indicated moderate potency of **27** with ORAC value 4.29 ± 0.19 trolox eq. Further, **27** demonstrated modest inhibition potency of $A\beta_{1-42}$ aggregation inhibition (65.6 ± 0.9%). Furthermore, compound **27** was found to be the most potent candidate in this series showing promising outcomes with Aβ anti-aggregation properties and acceptable BBB permeability. In addition, the selectivity and efficacy of these compounds against BChE indicated that these derivatives might be acting as a potential therapeutic agent for intermediate stages of AD.

2.5.2.3. FA-ethylenediamine tacrine derivatives

The research work of Digiacomo et al., 2015 [140], implicated that the insertion of 1,3-diamino-2-propanol spacer between the **FA** and tacrine improved the pharmacological profile of the developed hybrid compared to previously reported tacrine–DA (TAnFA) and tacrine–caffeic acid hybrids (TAnCA). Most of the designed compounds showed potent AChE inhibitory activity. The assessment of ChEI of the developed hybrids indicated the compound containing Chloro-substitution at 6^{th} position in the tetrahydroacridine fragment **29** (Figure 2.5) exhibits improved AChE inhibitory activity (IC_{50}= 0.15 μM) and selectivity towards AChE over BChE, relative to non-substituted derivative, for instance, **28** (Figure 2.5) with an IC_{50} value of 0.70 μM against AChE. Furthermore, in $A\beta_{1-42}$ modulation studies **28** and **29** showed 49.8% and 53.2% inhibition, respectively, at 50 μM towards Aβ self-aggregation. Compound **29** also presented potent antioxidant activity in DPPH assay (90.36 ± 1.4 % inhibition at 30 μM), promising metal (Cu^{2+}) chelation activity, and neuroprotective effect against glutamate-mediated cell death in HT22 cells with low toxicity profile, delineate a multifunctional profile of the developed hybrid.

2.5.2.4. FA-tacrine-melatonin hybrids (FATMHs)

Bencheroun *et al.*, 2016 [108] proposed tacrine multifunctional hybrids derived based on the conjunction of **FA**, formaldehyde, and a melatonin isocyanide in which melatonin and **FA** were selected for antioxidant property and tacrine was chosen for ChEs inhibition. **FA**-tacrine-melatonin hybrids (FATMHs) **30-31** (Figure 2.5) were biologically evaluated for their potential as ChE inhibitors and protective effect against ROS and Aβ species induced toxicity. Among the developed hybrids, **30** (Figure 2.5) containing **FA**-heptane alkyl chain linking to *N-1*-(7-methoxy 1,2,3,4-tetrahydroacridin-9-yl) moiety recognized as a most potential hybrid, exhibiting potent ChE inhibitory activity with IC_{50} = 1290 ± 70 nM against *h*AChE and IC_{50} = 234 ± 8 nM against *h*BChE with 5.5 fold selectivity over *h*AChE. *In-silico* studies were carried out to understand the binding interactions of hybrid **30** on *h*AChE (PDB # 4EY7) and *tc*AChE (PDB # 2ECK), and results pointed out the dual binding interaction at the PAS and CAS of AChE, similar to that found for bis (7)-tacrine. These hybrid molecules' neuroprotective profile was evaluated in neurotoxicity models induced through a mixture of oligomycin A and rotenone (O/R, respiratory chain blockers), H_2O_2 mediated ROS generation, and $A\beta_{1-40}$/$A\beta_{1-42}$ induced neurotoxicity.

Interestingly, compound **30** (at the dose of 3 μM) was identified to possess a significant neuroprotective profile against $A\beta_{1-40}$, $A\beta_{1-42}$ (70.6 and 81.4% %, respectively), and H_2O_2 (30.9%) mediated toxicity but marginal protective effect against toxicity induced by O/R and $A\beta_{1-40}$ species. Conversely, **31** (at the dose of 1 μM) (Figure 2.5) showed the highest protective effect against O/R and $A\beta_{1-42}$ induced toxicity (59.6 and 78.9%, respectively). The possible Nrf2-AREc activating impact of **30** and **31** was tested to get an insight into the mechanism of neuroprotection. The compound **31** had the most potent Nrf2 induction capability, followed by **30** with a concentration

needed to double the specific luciferase reporter activity (CD) value of 5.99 and 6.31 μM, respectively.

2.5.2.5. FA-tacrine piperazine amine side chain hybrids

Fu Y. *et al*. [141] in 2016, rationally designed and synthesized a series of novel **FA**-tacrine piperazine trihybrids by conjoining them with alkyl chain linkage, as shown in figure 2.5. All the synthesized compounds were assessed for their ChE inhibitory potency toward AChE, BChE, and self-induced Aβ aggregation inhibition. The SAR studies revealed **32** as the most potent among the developed compounds. The best inhibition was demonstrated by **32** with a 5-carbon spacer between **FA** and piperidine moiety (IC_{50} = 61.7 nM and 106.9 nM for AChE and BChE). Furthermore, the active compounds were also tested for modulation of $A\beta_{1-42}$ peptide, and protective effects on Aβ induced Neuro-2A cell injury.

2.5.2.6. FA tacrine-nitric oxide donor (NO) tri hybrid derivatives

In another series, Chen Y. *et al*., [142] developed and tested trihybrid derivatives constituted from **FA**-tacrine, and a nitric oxide donor (NO) fragments substituted at 4-hydroxy of phenyl ring into **FA** fragment to release nitric oxide and thereby confer vasodilatation properties. Raising evidence of experimental data suggested that incorporating NO donor fragments can be advantageous in the effective management of AD by increasing cerebral blood supply. In this series, the fusion of **FA**, tacrine, and nitric oxide donor was executed to address various factors involved in AD progression (Figure 2.5). They rationalized that the hybrid compounds should possess ChE inhibition and potent vasodilator potency due to the release of nitric oxide (NO). The effective anti-ChEs activity (in the nM range) was observed for all the tested derivatives. The ChE inhibition assay revealed that **33** (Figure 2.5) exhibited potent ChE inhibition (IC_{50} of AChE = 10.9 nM; IC_{50} of BChE = 17.7 nM) as compared to other compounds in this series. The SAR study revealed that the length

of the diamine side chain attached to the tacrine skeleton of the hybrids significantly influenced the ability to inhibit ChE. In the DPPH assay, it was observed that these derivatives exhibited less than 1% free radical scavenging activities at 2 mM concentration compared to parent moiety **FA** (100%), which delineate the role of free phenolic hydroxy groups of **FA** in conferring antioxidant property. Furthermore, the introduction of nitric oxide group significantly increased ChE inhibitory activity. Moreover, the most active compound **33** was also tested for its acute toxicity and scopolamine-induced mice amnesia model. The trihybrid **33** displayed substantial improvements in cognition profile in scopolamine-induced amnesia mice model and exhibited relatively less hepatotoxicity than parent moiety tacrine (Table 2.2).

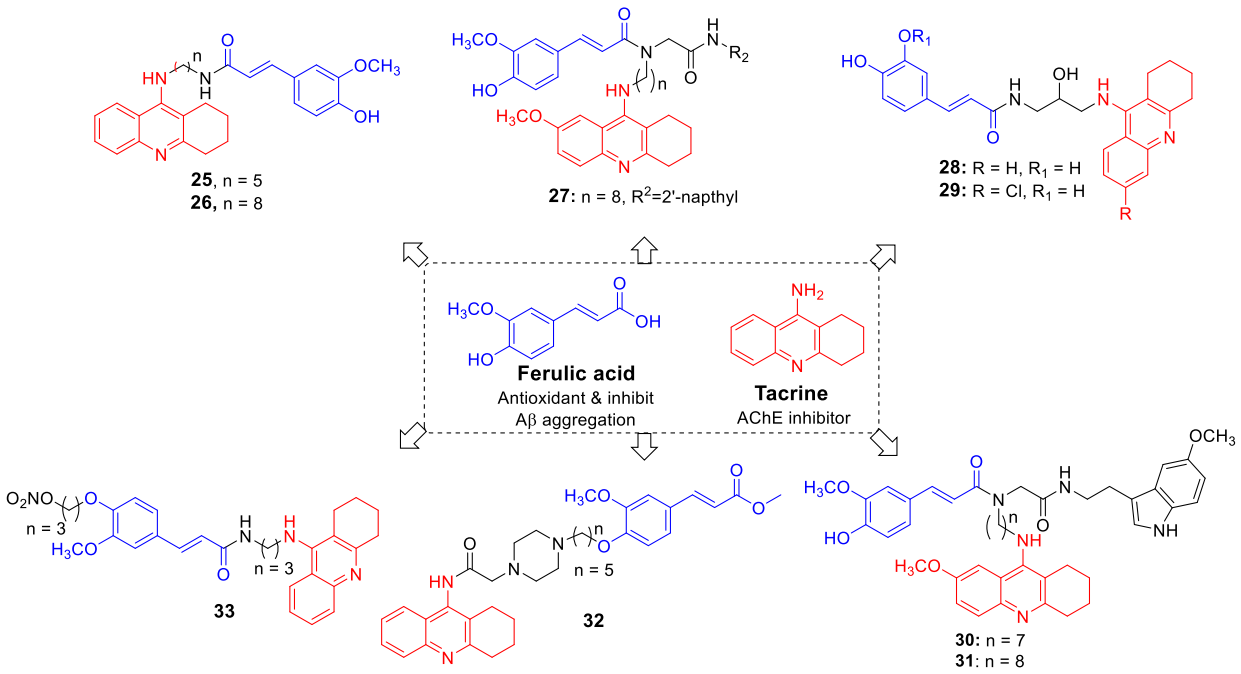

Figure 2.5. Chemical structures of **FA**-Tacrine derived hybrid molecules.

Table 2.2. *In-vitro* biological data for the evaluation of the therapeutic potential of hybrid analogs based on novel **FA**-tacrine-based hybrid analogs and their mode of action in the experimental AD model.

Sr. No.	Code	Pharmacological assessment of efficacy and safety				Mode of action	Ref.
		Cholinesterase inhibition (IC_{50}) ± SD		Neuroprotective activity	Antioxidant assay		
		AChE	BChE				
1	**25, 26**	4.4 ± 1.7 nM (25; *ee*AChE) 9.6 ± 2.1 nM (26; *ee*AChE)	6.7 ± 1.6 nM (25; *ee*BChE) 12.7 ± 2.6 nM (26; *ee*BChE)	*nd.*	ORAC value: 1.5 ± 0.01 TE for 25 and 1.4 ± 0.04 TE for 26.	ChEI activity, antioxidant, neuroprotective activity	[138]
2	**27**	22.2 ± 1.6 nM (27; *h*AChE)	68.2 ± 3.9 nM (27; *h*BChE)	59.4% cell viability (1000 μM; HepG2 cells) Aβ anti-aggregation activity : 65.6% (50 μM)	ORAC value: 4.29 ± 0.19 TE	ChEI activity, antioxidant, neuroprotective activity, Aβ modulator activity	[139]
3	**28, 29**	0.70 μM (28) 0.15 μM (29)	1.01 μM (28) 0.36 μM (29)	Aβ anti-aggregation activity : 53.2% (28; 50 μM) 49.8% (29; 50 μM)	*nd.*	ChEI activity, neuroprotective activity in glutamate-induced neuronal cell death in HT22 cells, metal chelating activity	[143]
4	**30, 31**	1290 ± 70 nM (30; *h*AChE) >10000 nM (31; *h*AChE)	234 ± 8 nM (30; *h*BChE) 336 ± 12 nM (31; *h*BChE)	68.7% ± 3.35 cell viability for 30 and 54.4% ± 0.94 for 31 (1000 μM; HepG2 cells)/ Aβ anti-aggregation activity : 81.4% (30; 3 μM) and 28.0% ± 3.19 (31; 3 μM)	ORAC value: 9.11 ± 0.21 TE for 30 and 7.27 ± 0.17 TE for 31	ChEI activity , neuroprotective potency, reduces H_2O_2 mediated ROS generation, cytoprotective activity against $A\beta_{1-40}$ /$A\beta_{1-42}$ induced neurotoxicity, Nrf2 induction capability	[108]

7	**32**	61.7 nM	106.9 nM	Aβ anti-aggregation activity :37.2% ± 0.9	*nd.*	ChEI activity, modulation of $A\beta_{1-42}$ peptide and protective effects on Aβ induced cell injury in Neuro-2A cell line.	[141]
8	**33**	10.9 nM (33)	17.7 nM (33)	*nd.*	*nd.*	ChEI activity, neuroprotective activity, no acute toxicity and improve memory in scopolamine-induced mice amnesia model.	[142]
9	**34**	19.7 ± 0.4 nM (34; *h*AChE)	0.59 ± 0.05 μM (34; *h*BChE)	Aβ anti-aggregation activity : 49.2% at 20 μM	ABTS* assay: 1.26 TE	ChEI activity, neuroprotective activity,$A\beta_{1-42}$ self-induced aggregation	[125]

IC_{50}: 50% inhibitory concentration (means ± SD of three experiments), *nd.* = not determined, *ee* = electric eel, *eq* = equine, *h* = human, *Data expressed in Trolox equivalent (TE), ** represented data of DPPH assay in IC_{50} ± SEM (n = 3).*

2.5.3. FA-rivastigmine derivatives

Recently in 2020, Lan *et al.,* [125] developed a series of compounds derived from **FA**, benzyl amino group, and carbomyl fragments from rivastigmine, a well known pseudo irreversible inhibitor of AChE and BChE, as MTDLs. The compound **34** (Figure 2.6) showed the most prominent activities towards cholinesterase inhibition with an IC_{50} value of 19.7 and 0.66 nM for *h*AChE and *h*BChE, respectively. The *in-vitro* biological studies identified **34** (49.2% at 20 μM) as the most effective inhibitor towards $A\beta_{1\text{-}42}$ self-induced aggregation, which indicated hydroxyl and methoxy groups might be beneficial for inhibition of Aβ aggregation. In the ABTS assay, **34** exhibited the highest antioxidant property with 1.26 trolox equivalents comparable to **FA** (1.12 trolox equivalents). Apart from these, **34** demonstrated neuroprotective activity against H_2O_2 induced oxidative stress model in PC12, and BBB penetration evaluated by PAMPA-BBB assay, which further potentiates therapeutic value of the designed derivative as MTDL (Table 2.2).

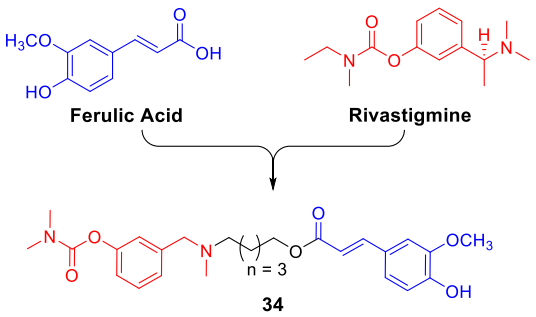

Figure 2.6. Chemical structures of **FA**-rivastigmine based hybrid molecules.

2.5.4. FA-N-benzyl-piperidine and N, N-dibenzyl (N-methyl) amine derivatives

Estrada *et al.* in 2016, [144] developed the compounds family based on the *N*-benzylpiperidine (NBP) and N, N-dibenzyl (N-methyl) amine (DBMA). The fragment NBP from DPZ was coupled with various substituted caffeic acid (CA) to generate compound **35** (Figure 2.7), and fragment DBMA from well-known AChE inhibitors 3-(4-((benzyl(methyl)amino) methyl)phenyl)-6,7-

dimethoxy-2*H*-chromen-2-one (AP2238) coupled with various substituted CA to generate compound **36** (Figure 2.7). The developed compounds were evaluated for neurogenic and neuroprotection properties in the AD model. The reaction between NBP and **CA** in carbonyl diimidazole (CDI) mediated amide coupling produced FA-NBP derivatives**.** The preliminary biological data based on *h*ChEs inhibition assay revealed moderate inhibitory activity of NBP-CA derivatives towards both isoforms, with a slightly higher preference for *h*AChE. Among the developed molecules, **35** exhibited *h*AChE inhibitory activity in low μM concentration (IC_{50} = 0.39 ± 0.05 μM) with unexpectedly preferential inversed *h*BChE inhibitory (IC_{50} = 76 nM) activity than the rest of its congeners. While the counterpart of NBP-CA**,** series *i.e.* DBMA-CA **(36)** hybrid retained inhibitory activity towards *h*AChE (IC_{50} = 3.49 ± 0.31 μM), but severely decreased *h*BChE inhibition potency (46% inhibition). Thus, the DBMA-CA hybrids displayed higher selectivity towards *h*AChE than the NBP-CA hybrid series. Compound **35** was found to be superior in inhibition (IC_{50} = 0.076 ± 0.01 μM) of *h*BChE over DPZ (IC_{50} = 2.50 ± 0.07 μM).

2.5.5. FA and memantine derivatives

In 2019, Rosini *et al.*, [145] designed and generated a series of compounds targeting ionotropic glutamate receptors *i.e.* N-methyl-D-aspartate receptors (NMDAR) activity which is responsible for maintaining synaptic plasticity in the healthy brain [146]. Memantine is a well-known FDA-approved anti-AD medication commercially available for the treatment of mild to severe forms of AD. It selectively targets the extra-synaptic NMDAR, which is hypothesized to trigger neuronal death mediated by Aβ [147]. In this research, the conjugation of memantine and **FA** hybrid derivatives were designed and synthesized to generate multifunctional molecules to protect the brain from Aβ mediated neuronal cell death and ROS-induced neurotoxicity. The NMDAR blocking activity was determined by voltage-clamp recordings on GluN1-1a/GluN2A NMDAR

expressed in Xenopuslaevis oocytes at -60 mV using memantine as a reference drug. The inhibition potency towards NMDAR depends on the linker length of the alkyl chain; for instance, compound **37** (Figure 2.7) with hexamethylene spacer showed the highest inhibition potency towards NMDAR with IC_{50} = 6.9 μM. Compound **37** was also assessed for voltage-dependent behavior *via* measuring the NMDA/glycine responses mediated by GluN1-1a/GluN2A at four different (-40, -60, -80, and -100 mV) holding potentials. The resultant data suggested that **39** slightly higher δ value (0.43 ± 0.12) properties as compared to memantine (δ value 0.39 ± 0.08) and property to act as open channel blockers of the receptor. The impact of scavenger on H_2O_2-induced damage in SH-SY5Y cells was evaluated using **FA** and dichlorodihydrofluorescein diacetate (DCFH-DA) revealed significant free radical scavenging effect of **37** effect. Furthermore, **37** could potentiate the nuclear factor (erythroid-derived 2)-like 2 (Nrf2) and its downstream protective gene heme oxygenase-1 (HO-1), a prototypical Nrf2-targeted gene responsible for oxidative stress in SH-SY5Y cells. Compound **37** significantly enhanced soluble amyloid precursor protein α (sAPPα) levels in H4-SW cells, which implicated the potential impact of trigger APP processing instead of activation of non-amyloidogenic (α-secretase) pathway and inhibition of Aβ aggregation.

2.5.6. FA-isoquinoline hybrids

Based on MTDLs strategy to combat AD, in 2019, Sang Z. *et al.*, [114] developed a novel series of **FA** derivatives coupled with substituted 1,2,3,4-tetrahydroisoquinoline moiety. In the *in-vitro* inhibitory studies, **38** (Figure 2.7)**,** demonstrated highest inhibitory activity with IC_{50} = 8.9 nM for BChE and remarkable inhibitory potency against MAO-A (IC_{50} = 6.3 μM) & MAO-B (IC_{50} = 8.6 μM). Compound **38** exhibited 59.3% inhibitory activity towards aggregation and 43.8% disaggregation property against self-induced amyloid β (Aβ) aggregation. Also, **38** produced significant anti-ROS activity with ORAC = 0.52 eq. Furthermore, **38** exhibited limited acute

toxicity and efficient brain permeability. In the zebrafish AD model, **38** demonstrated a favorable recovery rate in $AlCl_3$-induced dyskinesia and a potent neuroprotective effect on vascular injury induced by $A\beta_{1\text{-}40}$ (Table 2.3).

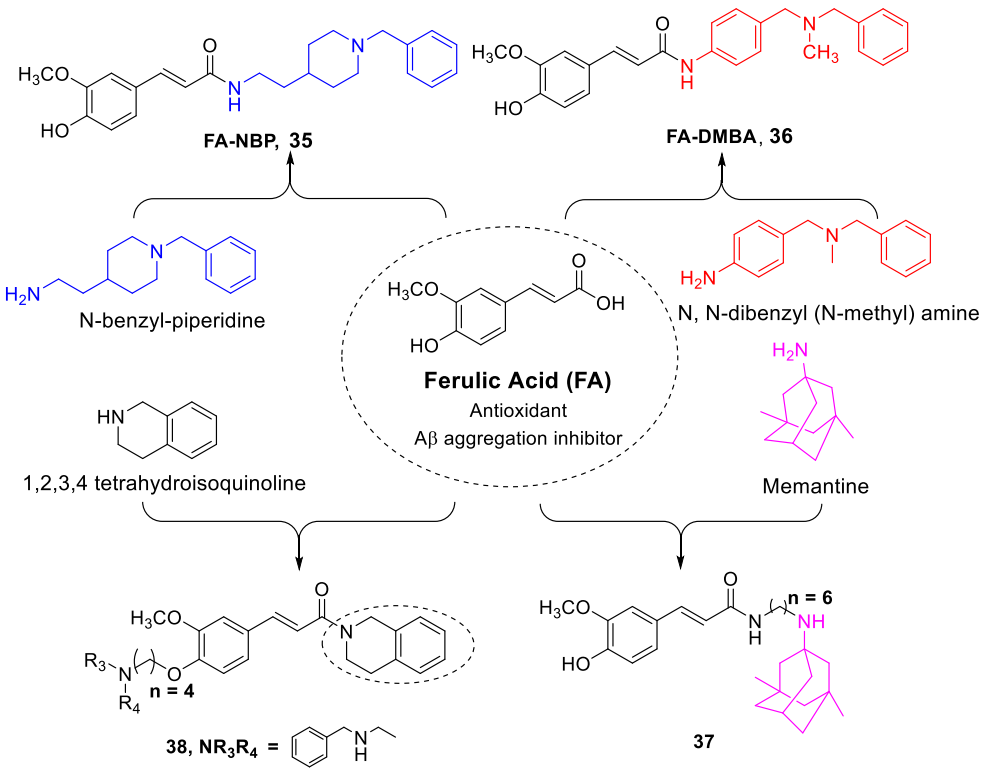

Figure 2.7. Chemical structures of various developed potent hybrids based on ferulamide derivatives of NBP, DMBA, tetrahydroisoquinoline and memantine.

2.5.7. Ferulic Acid-*O*-carbamoyl ferulamide derivative

Recently, Sang Z.*et al.* [148] reported another series of 21 novel compounds having *O*-carbamoyl ferulamide core based on MDTLs strategy and evaluated neuroprotective activity in the AD model. Most of the synthesized compounds showed significant inhibitory properties towards *ee*AChE and *eq*BChE. The removal of the methoxy group of **FA** fragment in the developed molecule **39** (IC_{50} = 0.92 μM) resulted in **40** (IC_{50} = 3.8 μM), which was found to be less potent against *eq*BChE compared to **39** (Figure 2.8). The role of 1,2,3,4-tetrahydroisoquinoline substitution in ChE

inhibition was further evaluated in molecular modeling studies. In *in-vitro* inhibitory studies, **39** had the strongest pseudo-irreversible *h*BChE inhibition (IC_{50} = 0.92 μM) potency with a selectivity index (SI) value 12.3. Also, it exhibited remarkable MAO-B inhibitory activity with an IC_{50} value of 5.3 μM. Moreover, **39** exhibited 58.2% inhibitory activity towards Aβ aggregation and 43.3% disaggregation property against self-induced $A\beta_{1-42}$ aggregation. The derivative **40** showed significant inhibitory activity towards self-induced aggregation in $A\beta_{1-42}$ with 52.9% inhibition at 25 μM. In the *in-vivo* zebrafish AD model, **39** demonstrated a desirable rate of recovery in $AlCl_3$-induced dyskinesia and potent neuroprotective effect on vascular injury induced by amyloid species ($A\beta_{1-40}$). In the [^{11}C]-radio-labelled PET-CT imaging derivative **39** exhibited brain permeability and rapid brain uptake after intravenous bolus injection. Compound **39** showed neuroprotection in Aβ induced neurotoxicity in SH-SY5Y cell line. Furthermore, **39** could reduce pathogenic tau levels accompanied by an increase in APP clearance rate and improve cognitive impairment in the scopolamine-induced model.

2.5.8. FA–carbazole hybrid derivatives

To achieve synergistic activity derived from the **FA** and carbazole moieties (ChE inhibitory activity), Fang L. *et al*., [149] developed a series of carbazole-**FA** hybrids coupled through amide linkage as novel multifunctional anti-AD agents. These hybrid compounds in Ellman's assay exhibited moderate to potent cholinesterases (ChEs) inhibitory activity. The SAR analysis concluded that a carbazole moiety substituted with an electron-withdrawing group and a side-chain with a small alkyl substituent favored ChE inhibition activity. *In-vitro* cholinesterase (*h*AChE and *h*BChE) inhibitory activities and antioxidant assays of the developed **FA**–carbazole hybrids were performed to evaluate neuroprotective efficacy. Among the developed hybrids, compound **42** (Figure 2.8) showed potent *ee*AChE (IC_{50} = 2.1 ± 0.6 μM) and *h*AChE (IC_{50} = 5.1 ± 0.8 μM)

inhibitory activity. In the enzyme inhibition studies against *eq*BChE and *h*BChE, **42** showed significant inhibitory activity with IC_{50} = 1.9 ± 0.2 μM and IC_{50} = 7.9 ± 0.5 μM, respectively, wherease **41** displayed a much less inhibitory activity against *ee*AChE (IC_{50} = 11.1 ± 2.4 μM) and *h*BChE (IC_{50} = 9.0 ± 2.1 μM) (Figure 2.8). In *in-vitro* DPPH-FRSA assay, **41** and **42** showed 44.1 ± 5.1%, and 41.8 ± 4.2% inhibition, respectively, at 1 μM, which confirmed the significant antioxidant property of the developed compounds. A comparative study of the therapeutic effect of the hybrid compound and its corresponding mixture (carbazole + **FA**) indicated that the therapeutic efficacy of the hybrid compound was greater compared to the mixture. Apart from this, **42** exhibited pronounced neuroprotective properties as an antioxidant agent in H_2O_2-induced toxicity.

2.5.9. FA-tertiary amine side chain derivatives

Liu H. *et al.* [126] in 2016 evaluated the significance of the phenolic hydroxyl group in designing a series of anti-AD drug molecules. Based on available literature on chalcone as potential AChE inhibitors, the design and synthesis of a series of novel **FA** benzamide derivatives with tertiary amine side chains were executed. Among the developed novel compounds, the majority exhibited potent AChE inhibitory activity than the standard drug rivastigmine (AChE IC_{50} = 10.54 ± 0.86 μmol/L and BChE IC_{50} = 0.26 ± 0.08 μmol/L). The benzamide-**FA**-O-alkylamine derivatives, **43** and **44** (Figure 2.8) exhibited most AChE inhibition potency with IC_{50} = 0.71 ± 0.08 μmol/L, and 1.11 ± 0.17 μmol/L, respectively. In terms of inhibition potency against BChE, **44** exhibited the most potent activity with IC_{50} = 2.23 ± 0.18 μmol/L. The SAR study suggested no significant impact on AChE inhibition activity with varying alkyl chain length in the phenolic hydroxyl group of **FA**. Still, a remarkable change in BChE inhibition property was observed.

2.5.10. FA-mamoquin hybrid

Pan W.*et al.,* [150] reported a series of novel multipotent derivatives sharing structural scaffold of **FA**-memoquin based hybrids and evaluated their biological potency as multifunctional anti-AD agents. Among the synthesized compounds, most of the agents demonstrated a significant AChE inhibition potency (IC_{50} = 3.2-34.7 μM), inhibition towards the self-induced $A\beta_{1-42}$ aggregation $A\beta_{1-42}$ (30.8-39.1%) at 25 μM, and exhibited potential antioxidant property (0.9-1.3 ORAC-FL values). In particular, compound **45** (Figure 2.8) was revealed as a lead derivative and displayed significant *ee*AChE inhibition potency (IC_{50} = 3.2 ± 0.02 μM) and 36.2% inhibition of BChE at 50 μM, as well as dose-dependent inhibitory effect on $A\beta_{1-42}$ aggregates (49.3%, 38.1%, and 26.8 ± 0.02 at 50, 25 and 10 μM). Disaggregation of self-induced $A\beta_{1-42}$ aggregates (45.5 ± 0.03%) at 25 μM of **45** further potentiates its efficacy against AD treatment. Additionally, in cytotoxicity study **45** showed 98.3± 1.8% cell viability at 10 μM in SH-SY5Y neuronal cell line, indicating the therapeutic safety of the target compound at 10 μM. Furthermore, compound **45** also showed a neuroprotective effect with 88.3 ± 6.5 % cell viability against H_2O_2 induced PC12 cell injury at 10 μM (Table 2.3).

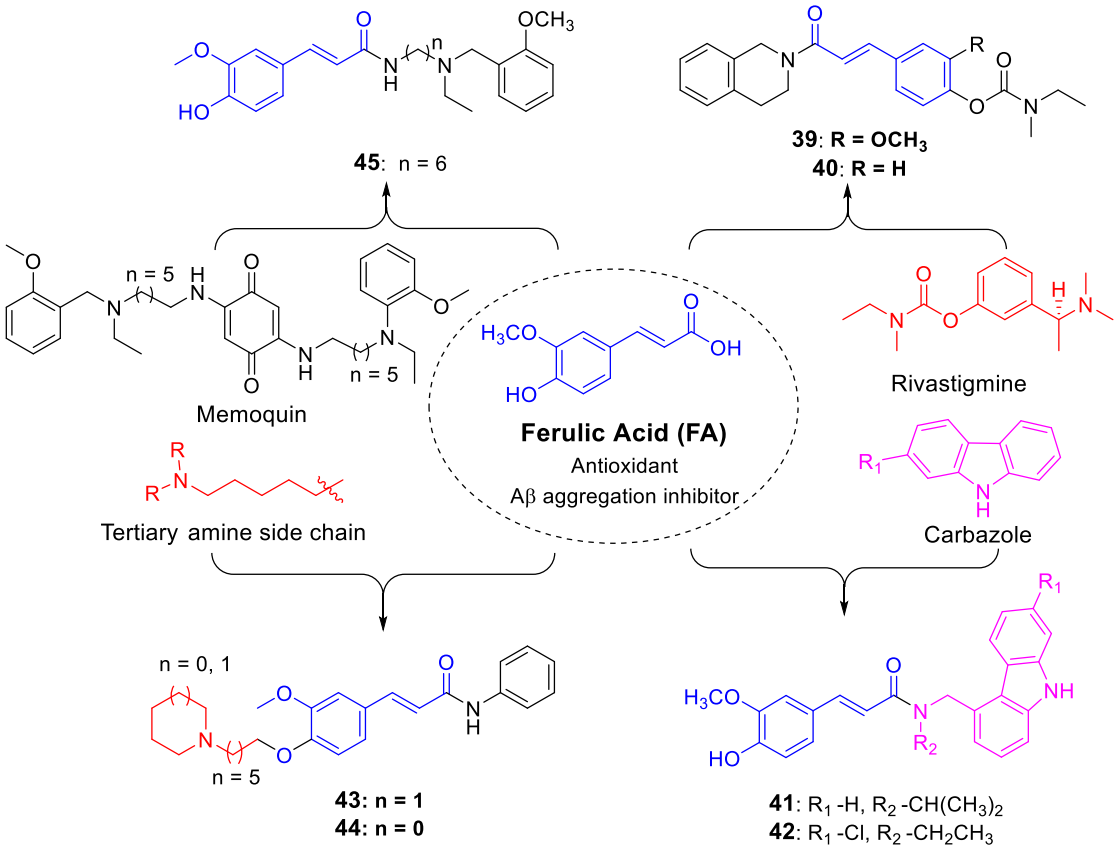

Figure 2.8. Chemical structures of potent **FA**-based hybrid analogs derived using fragments from memoquin, rivastigmine, carbazole, and tertiary amine side chain.

Table 2.3. *In-vitro* biological data for evaluating the therapeutic potential of hybrid analogs based on **FA** and their mode of action in the experimental AD model.

Sr. No.	Code	**Pharmacological assessment of efficacy and safety**				**Mode of action**	**Ref.**
		Cholinesterase inhibition (IC_{50}) ± SD		**Neuroprotective activity**	**Antioxidant assay**		
		AChE	**BChE**				
1	**35, 36**	0.39 ± 0.05 μM (35; *h*AChE) 5.99 ± 0.49 μM (36; *h*AChE)	0.076 ± 0.01 μM (35; *h*BChE) 5.89 ± 0.48 μM (36; *h*BChE)	MAO activity: 11.4 ± 0.4 μM (35; *h*MAO-A) 13.1 ± 0.8 μM (36; *h*MAO-B)	ORAC value: 1.8 ± 0.2 TE for 40 and 1.4 ± 0.11 TE for 36	ChEI activity, neuroprotective agent in AD mice model	[144]
2	**38**	12.1 ± 0.81 nM (38; *ee*AChE)	8.9 nM (38; *eq*BChE)	MAO activity: 6.3 ± 0.08[a] μM (MAO-A) & 8.6 ± 0.02 μM (MAO-B)[a] Amyloid β (Aβ) aggregation inhibition (59.3 %) and 43.8% disaggregation of Aβ aggregates	ORAC value: 0.52 ± 0.02 TE	ChEI activity, MAO inhibitor, Aβ aggregation inhibition, disintegrate preformed Aβ aggregates, neuroprotective agent, zebra fish AD model demonstrated favourable recovery rate in $AlCl_3$-induced dyskinesia	[114]
3	**39, 40**	11.3 ± 0.38 μM (39; *ee*AChE) 17.7 ± 0.43 μM (40; *ee*AChE)	0.92 ± 0.01μM (39; *eq*BChE) 3.8 ± 0.17μM (40; *eq*BChE)	MAO activity: 5.3 ± 0.22 μM (39; MAO-B) 15.9 ± 0.15 μM (39; MAO-A) 8.3 ± 0.34 μM (40; MAO-B) 97.3 ± 1.2 μM (40; MAO-A)	*nd.*	ChEI activity, MAO-B, neuroprotective agent, cyto-protective in Aβ induced SH-SY5Y cell line, zebra fish AD model demonstrated favourable recovery rate in $AlCl_3$-induced dyskinesia, improve cognitive impairment in scopolamine-induced model	[148]

4	**41, 42**	11.1 ±2.4 μM (41; *ee*AChE) 2.1 ± 0.6 μM (42; *ee*AChE)	12.7 ± 1.3 μM (41; *h*BChE) 1.9 ± 0.2 μM (42; *eq*BChE)	*nd.*	DPPH** assay: 90.9% ± 2.8 (41; 100 μM)	ChEI activity, antioxidant activity, neuroprotective effects against H_2O_2induced cell death	[149]
5	**43, 44**	0.71±0.08 μmol/L (43) 1.11±0.17 μmol/L (44)	12.97 ± 0.13 μmol/L (43) 2.23 ± 0.18 μmol/L (44)	*nd.*	*nd.*	ChEI activity, inhibition of self-induced amyloid $A\beta_{1-42}$ aggregation, preventing $A\beta_{1-42}$ and H_2O_2 induced toxicity on neuroblastoma cells	[126]
6	**45**	3.2 ± 0.02 μM	36.2%	49.3% inhibition of Aβ aggregation at 50 μM	ORAC value: 1.2 ± 0.01 TE	ChEI activity, inhibition of self-induced amyloid $A\beta_{1-42}$ aggregation, neuroprotective capacity in SH-SY5Y neuronal cell line and H_2O_2-induced PC12 cell injury	[150]

IC_{50}: 50% inhibitory concentration (means ± SD of three experiments), *nd.* = not determined, *ee* = electric eel, *eq* = equine, *h* = human [a]Monoamine oxidases (*h*MAO-A and *h*MAO-B) (IC_{50}, μM) *Data expressed in Trolox equivalent (TE), ** represented data of DPPH assay in IC_{50} ± SEM (n = 3).

2.5.11. Isosorbide-2-benzylcarbamate-5-ferulate or lipoic acid ester derivatives

Jones M. *et al.,* [151] presented a work on neuroprotective hybrids based on the hypothesis that the isosorbide-aryl-5-ester group could be replaced with an antioxidant functionality while retaining its selectivity and inhibition potency. The reported novel **FA** and LA esters coupled with isosorbide-2-benzylcarbamate derivatives as a potent antioxidant and selective BChE inhibitors. The 5-lipoate esters **46-49** (Figure 2.9) exhibited more promising inhibition of BChE than 5-ferulate esters **50-53 (**Figure 2.9) across the series. Notably, 2-benzyl carbamate (**46)** and butyl carbamate (**46**) of the 5-lipoates series exhibited the most potent BChE inhibitory property having IC_{50} of 150 and 170 nM, respectively. Among 5-ferulate esters, butyl carbamate derivative **52** exhibited BChE inhibitor potency with IC_{50} value 430 nM. In contrast, phenyl carbamate derivative of ferulate ester i.e. **51** had moderately potent AChE inhibitory activity (IC_{50} = 27.1 ± 11.3 μM) andlimited potency against BChE (IC_{50} = 29.16 μM). Among the developed compounds, against glutamate-induced neurotoxicity in HT-22 murine hippocampal cell line at 10-25 μM while, **FA** and the isosorbide-based 5-ferulate ester series *i.e.* **50**-**53**, were ineffective in protecting neuronal cells in the 1–25 μM range. Moreover, the tested compounds (**49** and **50**) displayed very weak antioxidant properties in the ORAC assay. The ORAC value of the isosorbide-2-phenylcarbamate-5-lipoic acid ester (**49**) was found insignificant (0.163 ± 0.146), whereas a weak yet significant effect was observed for isosorbide-2-benzylcarbanate-5-ferulate ester **50** with ORAC value 0.635 ± 0.020. The lack of activity of lipoate ester in non-cellular ORAC assay is not surprising as its anti-oxidant activity is primarily associated with cellular and mitochondrial-related processes.

2.5.12. FA and 1,3,4-oxadiazole derived hybrids

Tripathi *et al.* [152] designed and synthesized molecules based on FA and 1,3,4-oxadiazole to target multiple factors associated with AD. The developed compounds were screened against beta-secretase-1 (BACE-1), AChE, and BChE enzymes. Among the developed molecules, **54** and **55** (Figure 2.9) were found to be most potent and able to inhibit AChE (IC_{50} = 0.068 μM for **54** and 0.092 μM for **55**) and BChE (IC_{50} = 0.255 μM for **54** and 0.21 μM for **55**). Compounds **54** and **55** also exhibited BACE-1 inhibition properties with IC_{50} values of 0.25 μM and 0.21 μM, respectively. The BBB crossing ability was evaluated through PAMPA-BBB assay before testing the lead molecules in *in-vivo* AD animal models. Interestingly, the lead molecules were potent inhibitors of self-induced and AChE mediated Aβ aggregation along with the neuroprotective property against SH-SY5Y cells. In the *in-vivo* scopolamine-induced Y maze experiment, these compounds could reverse the cognitive dysfunction in mice. Further, *ex-vivo* estimation of the AChE level and the oxidative stress markers indicated the brain's AChE inhibition and potent antioxidant property of the lead compound **54**. Overall, **54** showed a better enhancement in learning and memory behavior in the Aβ-induced ICV rat model with an excellent oral absorption profile relative to **55**.

2.5.13. 7-*O*-Esters of taxifolin and FA derived hybrids

In 2020 S. Gunesch *et al.*,[153] used 7-*O*-ester hybrid of the flavonoid named taxifolin and incorporated it with **FA** *via* regio-selective synthesis to develop **56** and **57** (Figure 2.9). The synthesized derivatives exhibited neuroprotective ability towards a different form of cell death-called oxytosis and ferroptosis in murine hippocampal HT22 cells compared to taxifolin. Further, **56** and **57** were promising leads against ATP loss and significantly increased cell survival compared to taxifolin. Compound **56** showed a better survival rate (40% cell survival at 1 μM)

than taxifolin (10% cell survival at 1 μM) in HT22 cells. Further, it could also elevate the decreased level of total GSH due to the presence of glutamate. Furthermore, **56** demonstrated a decrease in bacterial lipopolysaccharide (LPS)-induced neuroinflammation in BV-2 mouse microglial cells by substantially decreasing the amount of IL-6 induction, NO production, and TNF-$\propto$. *In-vitro* finding indicated **56** and **57** have a significant over-additive effect relative to the mixture in an equivalent portion of **FA** with taxifolin (1:1). Finally, treatment with **56** and **57** could reverse Aβ induced memory deficit in mice and assumed to permeate BBB.

2.5.14. FA-quinolone hybrids

In 2019, Mo J.*et al.* [145] designed and synthesized **FA** and quinolone hybrid molecules. Among the synthesized molecules, **58** and **59** were the most potent AChE and BChE inhibitors (Figure 2.9). Compound **58** showed higher inhibition activity (IC_{50} = 0.62 ± 0.17 μM) towards AChE compared to **59** (IC_{50} = 3.28 ± 1.32 μM), whereas slightly lower inhibition activity of **58** towards BChE (IC_{50} = 1.18 ± 0.14 μM) compared to **59** (IC_{50} = 0.93 ± 0.40 μM) was observed. The compound **59** displayed greater radical quenching ability compared to **58** in the DPPH assay. Similarly, in the cytotoxicity studies, **59** was found to be devoid of toxicity in the HepG2 cell line and showed moderate neuroprotective activity against H_2O_2-induced oxidative stress in PC12 cells.

2.5.15. FA-berberine hybrid analogs

Berberine is a naturally available benzylisoquinoline alkaloids extracted from plants including *berberis vulgaris* and *Xanthorhiza simplicissima*. Several experimental evidence has shown the pathogenesis of extracellular amyloid plaques and intracellular neurofibrillary tangles in AD. In 2011, Zang *et al.,* [154] designed and synthesized a new series of hybrid molecules of **FA** and berberine analogs to develop MTDLs. The synthesized compounds were screened for their

biological activities for ChEs, Aβ aggregation inhibition, and antioxidant activity. The synthesized compounds had IC_{50} values in the range of 0.097-3.21 μM for AChE inhibition. It was further observed that **60** (Figure 2.9) could effectively inhibit AChE and BChE activities with IC_{50} value 3.21 ± 0.15 μM and 2.40 ± 0.04 μM, respectively. Furthermore, **60** displayed potent antioxidant activity (3.43 ± 0.11 Trolox equiv.) and could inhibit Aβ aggregation.

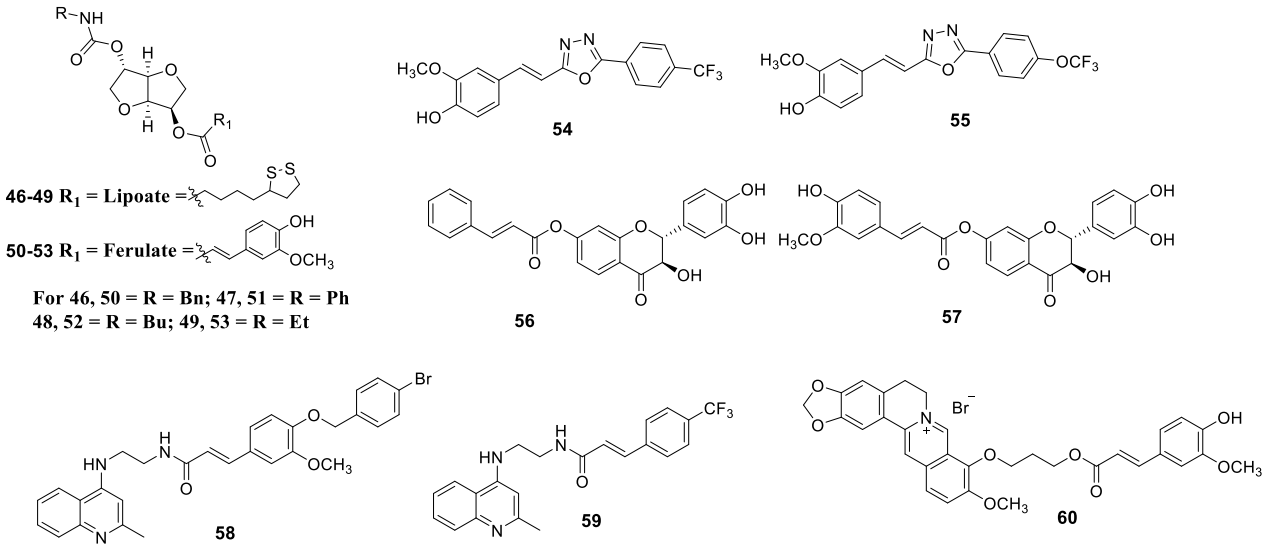

Figure 2.9. Chemical structures of multifunctional hybrid derivatives from various categories developed using ferulic acid structural architecture as potent cholinesterase inhibitors.